Traveling Wave Solutions of the Space-Time Fractional-Order Korteweg-de Vries Equation

Chao Li

***Abstract*—This paper investigates the space-time fractional-order Korteweg-de Vries (STFKdV) equation using dynamical systems and bifurcation theory. First, the STFKdV equation is transformed into a Hamiltonian system, and exact parametric expressions for its traveling wave solutions are derived. Subsequently, the paper also compares the space-time fractional-order and integer-order KdV equations, highlighting structural similarities and graphical differences, particularly influenced by the parameter λ. Finally, the theoretical methodology developed in this study is capable of addressing the solution of the entire spectrum of fractional-order KdV and integer-order equations with $p \in N^+$.**

***Index Terms*—Fractional-order; Traveling wave transformation; Hamiltonian system ; Exact solution.**

I. Introduction

IN the present work, a considerable amount of research activity has focused on nonlinear partial differential equations (NPDEs) (see [1]–[18]). Recently, numerous scholars have endeavored to explore the damped Korteweg-de Vries (KdV) equation

$$u_t + \beta u u_x + \mu u_{xxx} - \nu u_{xx} + v_x = 0, \quad \nu > 0, \tag{1}$$

where v is a forcing term and ν is a damping parameter. And its generalized form

$$u_t + \beta u^p u_x + \mu u_{xxx} - \nu u_{xx} + v_x = 0, \quad p > 0, \nu > 0. \tag{2}$$

Setting the parameters $v = 0$ and $\nu = 0$, the equation reverts to the unperturbed system

$$u_t + \beta u^p u_x + \mu u_{xxx} = 0, \quad p > 0. \tag{3}$$

In Eq. (1), (2) and (3), $u = u(x,t)$ and $v = v(x,t)$ represent the unknown functions dependent on the independent variables x and t. Meanwhile, p, μ, β and ν are real parameters.

In general, the Korteweg-de Vries equations are pivotal in the realms of mathematical physics, nonlinear theory, and their physical applications. Over the past few decades, numerous methodologies have been developed to address KdV equations [19]–[29]. Especially, Derks and Gilf [22] studied the uniqueness of traveling waves in perturbed KdV equations. Sun and Huang [28] proved that the KdV equations possess periodic waves with a fixed range of wave speed and established the coexistence of the solitary wave and one periodic wave. By analyzing the ratio of Abelian integrals, Chen et al. [29] proved that the limit wave speed of the general KdVs is decreasing and provided the upper and lower bounds of the limit wave speed. Liu et al. [30]–[32] transformed the variable-coefficient partial differential KdV equations into constant-coefficient KdV equations under some conditions by constructing equivalent transformations and presented the explicit solutions to the variable-coefficient KdVs in terms of the equivalent transformations.

Manuscript received August 1, 2024; revised April 1, 2025.

This work was supported by Fujian Key Laboratory of Big Data Application and Intellectualization for Tea Industry (Wuyi University) and the Natural Science Foundation of Fujian Province(No.2024J01321).

Chao Li is a lecturer of Mathematics and Computer, Wuyi University, Wuyi Shan, Fujian, P.C 354300, China, (e-mail: wyslch@wuyiu.edu.cn)

Drawing from the extensive scholarly work, we consider the conformable space-time fractional Korteweg-de Vries (STFKdV) equation, which is formulated as follows:

$$D_t^\alpha u + \beta u^p D_x^\lambda u + \mu D_x^\lambda D_x^\lambda D_x^\lambda u = 0, \ 0 < \alpha, \lambda \le 1. \tag{4}$$

In the Eq. (4), for the sake of convenience, let us assume that α, β, μ, λ are real constants and p is positive integer. And $D_t^\alpha u$ and $D_x^\lambda u$ are the conformable fractional derivative proposed by Khalil et al. [33]. If $\lambda = 1$, then STFKdV equation (4) degenerates into the time fractional-order KdV equation

$$D_t^\alpha u + \beta u^p u_x + \mu u_{xxx} = 0, \ 0 < \alpha \le 1. \tag{5}$$

Obviously,when $\alpha = 1$ and $\lambda = 1$, then STFKdV equation (4) becomes the integer-order KdV equation (3).

The paper is organized as follows. In Section II, the model be transformed into Hamiltonian system by traveling wave transformation. In Section III, we study the bifurcations and phase portraits of the Hamiltonian system. In Section IV, we present exact solutions of the Eq. (4) obtained respectively. In Section V, comparison between STFKdV equation and the integer-order KdV equation is presented. Finally, we conclude our paper in Section VI.

II. Transformation

In this section, we use the following transformation

$$u(x,t) = u(\eta), \qquad \eta = x^\lambda - l t^\alpha, \tag{6}$$

where l, which is positive, signifies the velocity at which the wave propagates. We obtain

$$D_t^\alpha u(x,t) = t^{1-\alpha} \frac{\partial u(x,t)}{\partial t} = t^{1-\alpha} \frac{du(\eta)}{d\eta} \frac{\partial \eta}{\partial t} = -l\alpha u', \tag{7}$$

$$D_x^\lambda u(x,t) = x^{1-\lambda} \frac{\partial u(x,t)}{\partial x} = x^{1-\lambda} \frac{du(\eta)}{d\eta} \frac{\partial \eta}{\partial x} = \lambda u', \tag{8}$$

$$D_x^\lambda D_x^\lambda D_x^\lambda u(x,t) = \lambda^3 u'''. \tag{9}$$

Substituting the above into the STFKdV equation, we derive the following ordinary differential equation:

$$-l\alpha u' + \beta \lambda u^p u' + \mu \lambda^3 u''' = 0. \tag{10}$$

Then, by integrating both sides of Eq. (10), we obtain the following equations:

$$-l\alpha u + \frac{\beta\lambda}{p+1} u^{p+1} + \mu\lambda^3 u'' = a, \tag{11}$$

$$u'' - \frac{l\alpha}{\mu\lambda^3}u + \frac{\beta}{\mu(p+1)\lambda^2}u^{p+1} = \frac{a}{\mu\lambda^3}, \tag{12}$$

where a is arbitrary constants. For convenience, posing $c = \frac{l\alpha}{\mu\lambda^3}$, $b = \frac{\beta}{\mu\lambda^2}$, $\delta = \frac{a}{\mu\lambda^3}$, transforms Eq. (11) to the following form:

$$u'' - cu + \frac{b}{p+1}u^{p+1} = \delta. \tag{13}$$

Now, let's talk about properties of Eq. (13) and transform it into Hamiltonian system

$$\begin{cases} \dfrac{du}{d\eta} = \Psi, \\ \dfrac{d\Psi}{d\eta} = cu - \dfrac{b}{p+1}u^{p+1} + \delta. \end{cases} \tag{14}$$

Additionally, the first integral is expressed as

$$H(u,\Psi) = \frac{1}{2}\Psi^2 - \frac{1}{2}cu^2 + \frac{b}{(p+1)(p+2)}u^{p+2} + \delta u = h. \tag{15}$$

Based on the analysis above, we reach the following theorem:

Theorem II.1. *The STFKdV equation (4) can be turn into a dynamical systems (14) by the traveling wave transformation (6).*

III. Bifurcations and phase portraits of dynamical system (14)

For further analysis, we need to discuss the equilibrium points of the Hamiltonian system (14). Let $\Gamma(u) = cu - \frac{b}{p+1}u^{p+1} + \delta$, then $\Gamma'(u) = c - bu^p$. Apparently, the roots of $\Gamma(u) = 0$ depend on the parameter set (p, c, b, δ). Through computation, we find:

1) If p is odd and $(\delta + d_0)b < 0$, then $\Gamma(u) = 0$ has no real root:
2) If one of the following cases is satisfied, then $\Gamma(u) = 0$ has only one real root u_1:
   - p is even and $bc < 0$;
   - p is even, $\delta \neq \pm d_0$, and $bc > 0$;
   - p is odd and $\delta = d_0$;
3) If one of the following cases is satisfied, then $\Gamma(u) = 0$ has two real roots u_2, $u_3 (u_3 < u_2)$:
   - p is odd and $(\delta + d_0) > 0$;
   - p is even, $\delta = \pm d_0$, and $bc > 0$;
4) If one of the following cases is satisfied, then $\Gamma(u) = 0$ has three real roots $u_4, u_5, u_6 (u_6 < u_5 < u_4)$:
   - p is even, $b < 0$, $c < 0$, and $d_0 < \delta < -d_0$;
   - p is even, $b > 0$, $c > 0$, and $-d_0 < \delta < d_0$;

where $d_0 = \frac{pc}{p+1}(\frac{c}{b})^{\frac{1}{p}}$.

Furthermore, note that

$$J(u_i, \Psi_i) = \det M(u_i, \Psi_i) = -\Gamma'(u) = -bu^p + c. \tag{16}$$

In the context of the linearized system derived from equation (14) at equilibrium points $E_i (i = 1, 2, \ldots, 6)$ $(E_i = (u_i, 0))$, the matrix of coefficients is denoted by $M(u_i, \Psi_i)$. By applying the equilibrium point theory (as detailed in reference [34]), the computation is readily executed to find that

a. $J(u_1, 0) > 0$ (indicating a center point), if p is even, $b > 0$, $c < 0$ or $b > 0$, $c > 0$, and $\delta \neq \pm d_0$; [as shown in Fig. 1(a)]

b. $J(u_1, 0) = 0$ (indicating a saddle point), if p is odd and $\delta = d_0$; [as shown in Fig. 1(b)]

c. $J(u_1, 0) < 0$ (indicating a cusp point), if p is even,$b < 0$, $c > 0$ or $b < 0$, $c < 0$, $\delta \neq \pm d_0$; [as shown in Fig. 1(c)]

d. $J(u_2, 0) > 0$ (indicating a center point), $J(u_3, 0) < 0$ (indicating a saddle point), if p is odd, $b > 0$, $\delta < -d_0$; [as shown in Fig. 1(d)]

e. $J(u_2, 0) < 0$ (indicating a saddle point), $J(u_3, 0) > 0$ (indicating a center point), if p is odd, $b < 0$, $\delta > -d_0$; [as shown in Fig. 1(e)]

f. $J(u_2, 0) < 0$ (indicating a saddle point), $J(u_3, 0) = 0$ (indicating a cusp point), if p is even, $b < 0$, $c < 0$, $\delta = d_0$; [as shown in Fig. 1(f)]

g. $J(u_2, 0) = 0$ (indicating a cusp point), $J(u_3, 0) < 0$ (indicating a saddle point), if p is even, $b < 0$, $c < 0$, $\delta = -d_0$; [as shown in Fig. 1(g)]

h. $J(u_2, 0) > 0$ (indicating a center point), $J(u_3, 0) = 0$ (indicating a cusp point), if p is even, $b > 0$, $c > 0$, $\delta = d_0$; [as shown in Fig. 1(h)]

i. $J(u_2, 0) = 0$ (indicating a cusp point), $J(u_3, 0) > 0$ (indicating a center point), if p is even, $b < 0$, $c < 0$, $\delta = -d_0$; [as shown in Fig. 1(i)]

j. $J(u_4, 0) < 0$ (indicating a saddle point), $J(u_5, 0) > 0$ (indicating a center point), $J(u_6, 0) < 0$ (indicating a saddle point), if p is even, $b < 0$, $c < 0$, $d_0 < \delta < -d_0$; [as shown in Fig. 1(j) and Fig. 1(l)]

g. $J(u_4, 0) > 0$ (indicating a center point), $J(u_5, 0) < 0$ (indicating a saddle point), $J(u_6, 0) > 0$ (indicating a center point), if p is even, $b > 0$, $c > 0$, $-d_0 < \delta < d_0$. [as shown in Fig. 1(k)]

It is evident that the system (14) exhibits more phase portraits when p is even compared to when p is odd .

IV. Exact solutions to the STFKdV equarion (4)

In this section, we identify the solutions of the Hamiltonian system (14). From the first integral, we establish the integral constant h as a fixed value, which results in

$$\begin{aligned} \Psi^2 &= cu^2 - \frac{2b}{(p+1)(p+2)}u^{p+2} + 2\delta u + 2h \\ &= \mid \frac{2b}{(p+1)(p+2)} \mid \Phi(u). \end{aligned} \tag{17}$$

The function $\Phi(u)$ represents a polynomial of the $(p+2)$th degree in the variable u.

$$\Psi^2 = \begin{cases} \frac{2b}{(p+1)(p+2)}\Phi(u), & b \geq 0, \\ -\frac{2b}{(p+1)(p+2)}\Phi(u), & b < 0. \end{cases} \tag{18}$$

Apparently, the number and types of equilibrium points of planar dynamical system (14) are affected by the parity of p. As the parity of p has an impact on the phase diagram of system (14), we will now engage in a classification discussion.

A. Case I: p is odd

In this section, we examine the case where p is an odd number. For the sake of simplicity, we presume $p = 1$. We now proceed to analyze the traveling wave solutions associated with the distinct bounded bifurcations of the phase

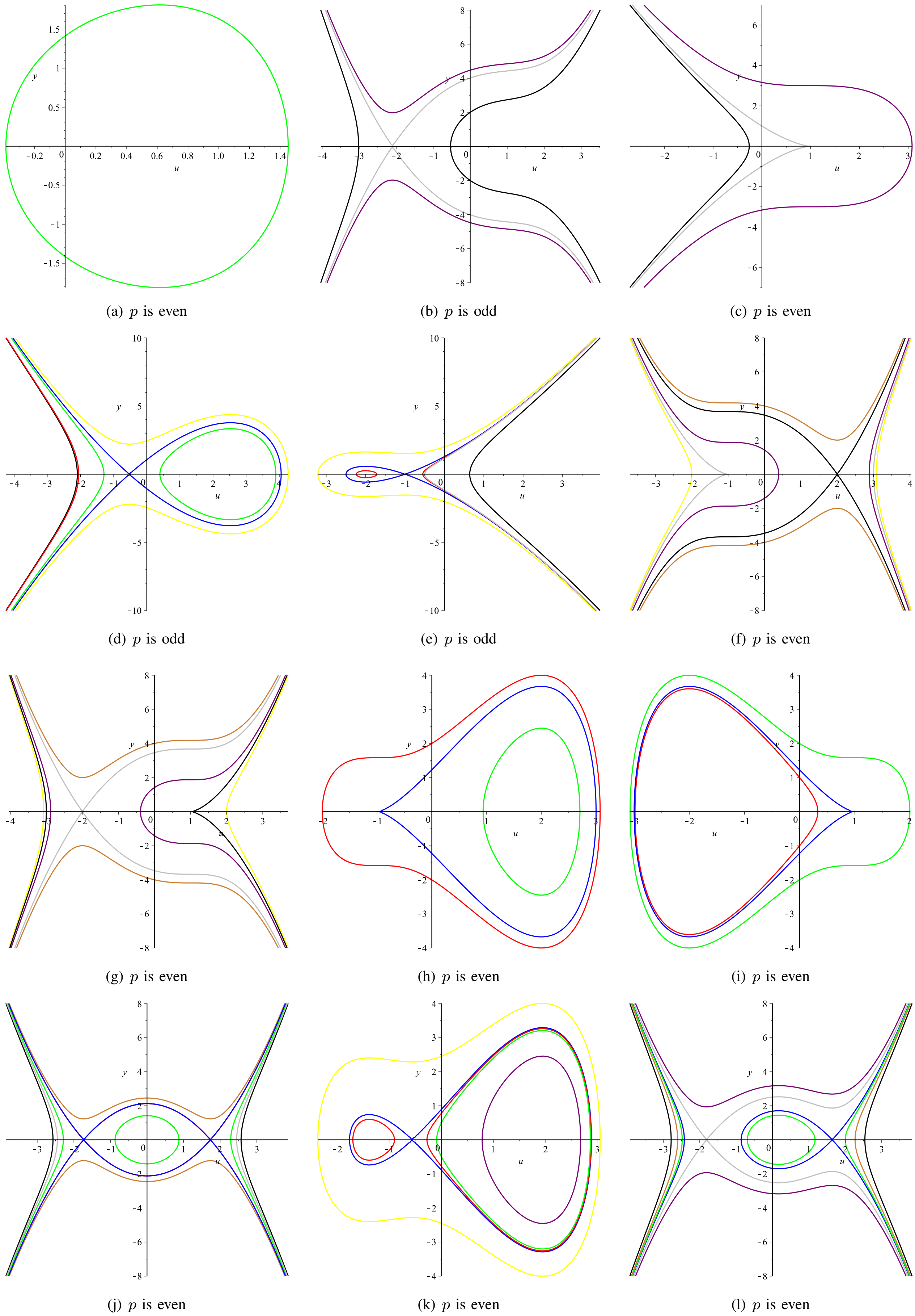

(a) p is even (b) p is odd (c) p is even

(d) p is odd (e) p is odd (f) p is even

(g) p is even (h) p is even (i) p is even

(j) p is even (k) p is even (l) p is even

Fig. 1: Bifurcations and phase portraits of the system (14).

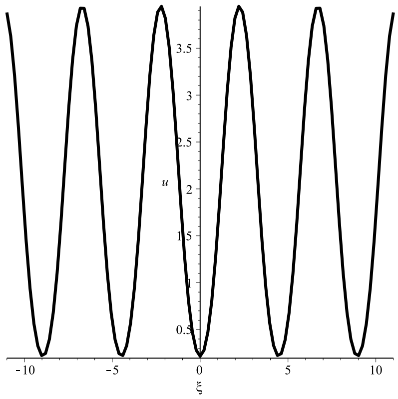

(a) Periodic wave of (14)

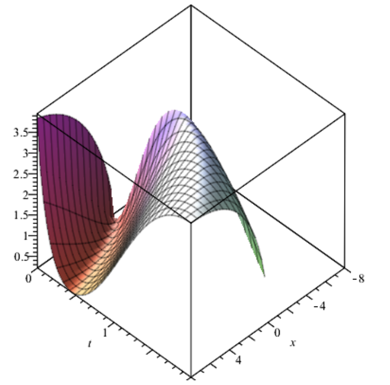

(b) Exact solutions of (4)

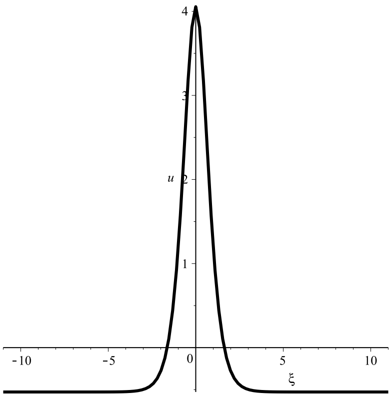

(c) Bright solitary wave of (14)

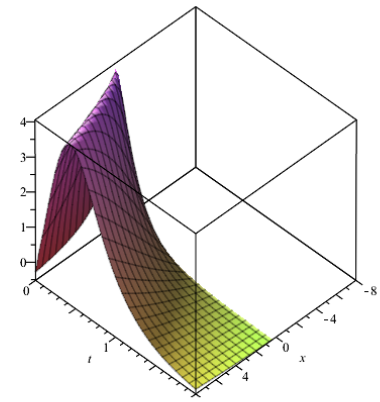

(d) Exact solutions of (4)

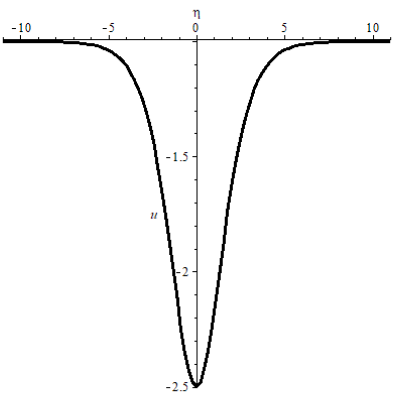

(e) Dark solitary wave of (14)

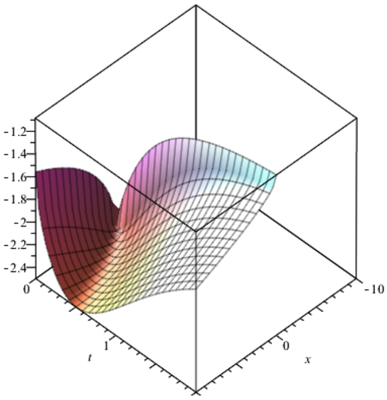

(f) Exact solutions of (4)

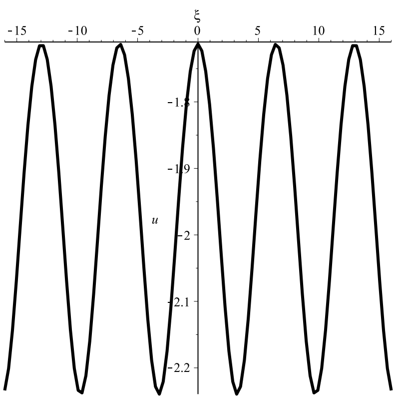

(g) Periodic wave of (14)

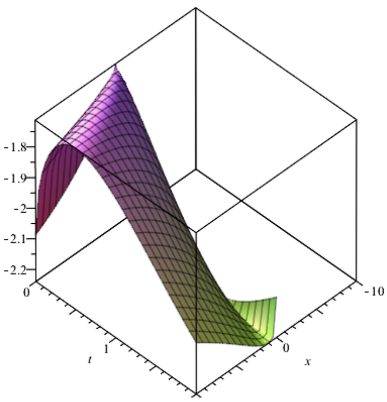

(h) Exact solutions of (4)

Fig. 2: Various waves of system (14) and graphs of solutions for (4) with $\alpha = \frac{1}{2}$, $\lambda = \frac{1}{3}$,$p = 1$

portraits depicted in Fig.1 (b) and Fig. 1(d). If $p = 1$, then the Eq. (17) is transformed into the following form

$$\Psi^2 = cu^2 - \frac{b}{3}u^3 + 2\delta u + 2h = \pm\frac{b}{3}\Phi(u). \quad (19)$$

In the formula (19), $\Phi(u)$ is defined as a three-degree polynomial in u. Integrating along a branch of the curve, starting from the initial value $u(t_0) = u_0$, yields us

$$\eta = \int_{u_0}^{u} \sqrt{\pm\frac{3}{b\Phi(s)}}ds. \quad (20)$$

Let $h_i = H(u_i, 0)(i = 1, 2, \ldots, 6)$, for the phase portraits, respectively.

Then we just consider the Fig. 2(a) as follows.

(i) Firstly, considering Fig. 1(d), we identify the green curve that represents a series of periodic orbits surrounding the equilibrium point $E_2(u_2, 0)$. These orbits exist within the range $h \in (h_2, h_3)$ and under the condition that b is positive Designating ξ_1, ξ_2, ξ_3 (with $\xi_3 < \xi_2 \le u < \xi_1$) intersection points of the green curve with the u-axis in Fig. 1(d), we proceed to write:

$$\Phi(u) = (\xi_1 - u)(u - \xi_2)(u - \xi_3). \quad (21)$$

From the formula (see 235.00 in [35]), we have

$$\begin{aligned} & \int_{\xi_2}^{u} \frac{ds}{\sqrt{(\xi_1 - s)(s - \xi_2)(s - \xi_3)}} \\ = \;& g\text{sn}^{-1}(\sin\varphi, k) \\ = \;& \sqrt{\frac{b}{3}}\eta, \end{aligned} \quad (22)$$

where $\varphi = \sin^{-1}\sqrt{\frac{(\xi_1-\xi_3)(u-\xi_2)}{(\xi_1-\xi_2)(u-\xi_3)}}$, $g = \frac{2}{\sqrt{(\xi_1-\xi_3)}}$, $k^2 = \frac{\xi_1-\xi_2}{\xi_1-\xi_3}$. Consequently, based on Eq. (22), it guides us to $\sin\varphi = \text{sn}(\frac{1}{g}\sqrt{\frac{b}{3}}\eta, k) = \sqrt{\frac{(\xi_1-\xi_3)(u-\xi_2)}{(\xi_1-\xi_2)(u-\xi_3)}}$. Therefore, the parametric formulation of the periodic trajectory of system (14) as depicted in Fig. 2(a), is presented as follows:

$$u(\eta) = \frac{\xi_3(\xi_1 - \xi_2)\text{sn}^2(\frac{1}{g}\sqrt{\frac{b}{3}}\eta, k) - \xi_1\xi_2 + \xi_2\xi_3}{(\xi_1 - \xi_2)\text{sn}^2(\frac{1}{g}\sqrt{\frac{b}{3}}\eta, k) - \xi_1 + \xi_3}. \quad (23)$$

Here $\text{sn}(\xi, k)$ denotes the elliptic sine function, which is a Jacobian elliptic function. Correspondingly, the precise periodic waveform solutions for Eq. (4), as illustrated in Fig. 2(b), can be articulated as:

$$u(x,t) = \frac{\xi_3(\xi_1 - \xi_2)\text{sn}^2(\frac{1}{g}\sqrt{\frac{b}{3}}(x^\lambda - lt^\alpha), k) - \xi_1\xi_2 + \xi_2\xi_3}{(\xi_1 - \xi_2)\text{sn}^2(\frac{1}{g}\sqrt{\frac{b}{3}}(x^\lambda - lt^\alpha), k) - \xi_1 + \xi_3}. \quad (24)$$

(ii) Secondly, if $h = h_2$, we get the blue level curve in Fig. 1(d). Currently, there is a homoclinic orbit encircling the equilibrium point $E_2(u_2, 0)$. Hence, the function $\Phi(u) = (u-\xi_2)^2(\xi_1-u)$ (ξ_1, ξ_2, with ξ_1 and ξ_2 being the coordinates where the blue curve intersects the u-axis as shown in Fig. 1(d). For values of u that satisfy $\xi_2 < u < \xi_1$, we then formulate

$$\begin{aligned} & \int_{u}^{\xi_1} \frac{ds}{\sqrt{(\xi_1 - s)(s - \xi_2)^2}} \\ = \;& \frac{1}{\sqrt{\xi_1 - \xi_2}}\ln\frac{\sqrt{\xi_1 - \xi_2} + \sqrt{\xi_1 - u}}{\sqrt{\xi_1 - \xi_2} - \sqrt{\xi_1 - u}} \\ = \;& \sqrt{\frac{3}{b}}\eta. \end{aligned} \quad (25)$$

Therefore, the parametric formulation of the homoclinic trajectory of system (14) as depicted in Fig. 2(c), is presented as follows:

$$u(\eta) = \xi_1 - [\frac{e^{\rho\eta} - 1}{e^{\rho\eta} + 1}]^2(\xi_1 - \xi_2), \quad (26)$$

where $\rho = \sqrt{\frac{b(\xi_1-\xi_2)}{3}}$. Hence, correspondingly, the precise bright solitary waveform solutions for Eq. (4), as illustrated in Fig. 2(d), can be articulated as:

$$u(x,t) = \xi_1 - [\frac{e^{\rho(x^\lambda - lt^\alpha)} - 1}{e^{\rho(x^\lambda - lt^\alpha)} + 1}]^2(\xi_1 - \xi_2). \quad (27)$$

Similarly, according to Fig. 1(e), we determine the precise parametric expression for the homoclinic orbit within system (14), as depicted in Fig. 2(e). We also identify the dark solitary wave solutions for Eq. (4), shown in Fig. 2(f), along with the parametric expression for the periodic orbit of system (14), illustrated in Fig. 2(g), and the exact periodic wave solutions for Eq. (4), as seen in Fig. 2(h).

$$u(\eta) = \xi_2 + [\frac{e^{\rho_1\eta} - 1}{e^{\rho_1\eta} + 1}]^2(\xi_1 - \xi_2), \quad (28)$$

$$u(x,t) = \xi_2 + [\frac{e^{\rho_1(x^\lambda - lt^\alpha)} - 1}{e^{\rho_1(x^\lambda - lt^\alpha)} + 1}]^2(\xi_1 - \xi_2), \quad (29)$$

$$u(\eta) = \frac{\xi_1(\xi_2 - \xi_3)\text{sn}^2(\frac{1}{g}\sqrt{-\frac{b}{3}}\eta, k_1) - \xi_1\xi_2 + \xi_2\xi_3}{(\xi_2 - \xi_3)\text{sn}^2(\frac{1}{g}\sqrt{1\frac{b}{3}}\eta, k_1) - \xi_1 + \xi_3}, \quad (30)$$

$$u(x,t) = \frac{\xi_1(\xi_2 - \xi_3)\text{sn}^2(\frac{1}{g}\sqrt{-\frac{b}{3}}(x^\lambda - lt^\alpha), k_1) - \xi_1\xi_2 + \xi_2\xi_3}{(\xi_2 - \xi_3)\text{sn}^2(\frac{1}{g}\sqrt{-\frac{b}{3}}(x^\lambda - lt^\alpha), k_1) - \xi_1 + \xi_3}, \quad (31)$$

where $\rho_1 = \sqrt{-\frac{b}{3}(\xi_1 - \xi_2)}$, $k_1^2 = \frac{\xi_2-\xi_3}{\xi_1-\xi_3}$.

Through the above analysis, we get the following conclusion:

Given that $p = 2n - 1$, the system (14) manifests periodic and solitary wave patterns. Concurrently, the STFKdV equation (4) presents a spectrum of solutions including periodic waves, as well as both dark and bright solitary waves.

B. Case II: p is even

The following section focuses on p is even. For ease of computation, we posit $p = 2$ and delve into the analysis of all traveling wave solutions associated with the various bounded bifurcations of phase portraits as previously outlined [Fig. 1(a), 2(e), 2(f), 3(a), 3(b) and 3(c)].

In a manner analogous to Case I, the traveling wave solutions for the STFKdV equation with $p = 2$ can be determined. In the current scenario, the system (14) not only features periodic waves, dark solitary waves, and bright solitary waves but also introduces kink waves. Concurrently, the

STFKdV equation encompass a range of solutions, including periodic waves, dark solitary waves, bright solitary waves, and additional kink wave solutions. The other cases will not be further discussed, and only the case of kink wave solutions will be presented here. Substituting $p = 2$ in the Eq. (17), gives us the following form:

$$\Psi^2 = cu^2 - \frac{b}{6}u^4 + 2du + 2h = \pm\frac{b}{6}\Phi(u). \tag{32}$$

In the preceding Eq. (32), $\Phi(u)$ is defined as a four-degree polynomial in u. We derive the solution by integrating over the corresponding curve from initial value $u(t_0) = u_0$,

$$\eta = \int_{u_0}^{u}\sqrt{\pm\frac{6}{b\Phi(s)}}ds. \tag{33}$$

If $h = h_4$ or $h = h_6$, we get the blue level curve in Fig. 3(a). Designate ξ_1 and ξ_2 as the coordinates where the red curve crosses the u-axis in Fig. 3(a). Now, it corresponds two heteroclinic orbits surrounding $E_5(u_5, 0)$. Thus, $\Phi(u) = (\xi_1 - u)^2(u - \xi_2)^2$, and $\xi_1 = -\xi_2$. When $\xi_2 < u < \xi_1$, then we obtain

$$\begin{aligned} & \int_0^u \frac{ds}{\sqrt{(\xi_1 - s)^2(s - \xi_2)^2}} \\ = & \int_0^u \frac{ds}{(\xi_1 - s)(s - \xi_2)} \\ = & \sqrt{-\frac{b}{6}}\eta. \end{aligned} \tag{34}$$

Therefore, the precise parametric formulation for the heteroclinic orbit of system (14), as derived from [refer to Fig. 10(a)], is given by

$$u(\eta) = \frac{\xi_1 e^{(\xi_1-\xi_2)\sqrt{-\frac{b}{6}}\eta} + \xi_2}{1 + e^{(\xi_1-\xi_2)\sqrt{-\frac{b}{6}}\eta}}. \tag{35}$$

Thus, in correspondence, we derive the kink wave solutions for Eq. (4) as detailed below [refer to Fig.(b)]:

$$u(x,t) = \frac{\xi_1 e^{(\xi_1-\xi_2)\sqrt{-\frac{b}{6}}(x^\lambda - lt^\alpha)} + \xi_2}{1 + e^{(\xi_1-\xi_2)\sqrt{-\frac{b}{6}}(x^\lambda - lt^\alpha)}}. \tag{36}$$

By synthesizing the discussions from the two previous cases, we arrive at the following theorem:

Theorem IV.1. *The fractional-order Korteweg-de Vries (STFKdV) equation (4) encompasses a variety of wave solutions, including kink waves, periodic waves, dark solitary waves, bright solitary waves, and additional kink wave solutions.*

V. Comparison between the STFKdV equation and the integer-order KdV equation

As discussed in Section I, the STFKdV equation (4) transforms into the integer-order KdV equation (3) when $\lambda = 1$ and $\alpha = 1$. Similarly, the integer-order KdV equation (3) can be reformulated into a dynamical system that mirrors the structure of system (14).

$$\begin{cases} \dfrac{du}{d\eta} = \Psi, \\ \frac{d\Psi}{d\eta} = \tilde{c}u - \frac{\tilde{b}}{p+1}u^{p+1} + \tilde{\delta}, \end{cases} \tag{37}$$

where $\tilde{c} = \frac{l}{\mu}$, $\tilde{b} = \frac{\beta}{\mu}$, $\delta = \frac{\tilde{a}}{\mu}$,and $\tilde{a}$ is arbitrary constants.

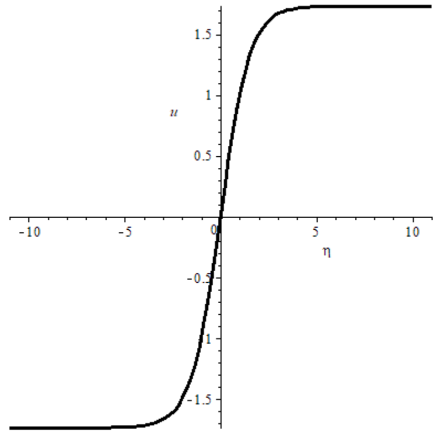

(a) Kink wave of (14)

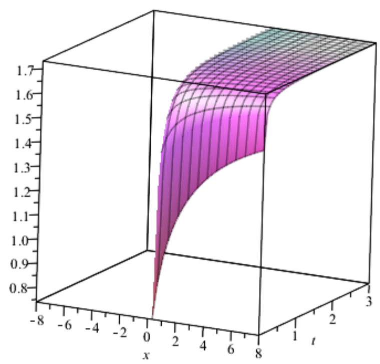

(b) Exact solutions of (4)

Fig. 3: Kink wave of system (14) and graph of solutions for (4) with $\alpha = \frac{1}{2}, \lambda = \frac{1}{3}, p = 2, b = -3, c = -3, \delta = 0$.

Subsequently, let us investigate the distinctions between the STFKdV equation and the integer-order KdV equation. In systems (14) and (37), letting $\tilde{c} = c$, $\tilde{b} = b$, $\delta = \delta$, provides us with a result that the newly derived dynamical system (37) and the Hamiltonian system (14) possess identical phase portraits (see Fig. 1). Consequently, As a result, it becomes evident that the integer-order KdV equation (3) includes a spectrum of solutions such as kink waves, periodic waves, dark solitary waves, bright solitary waves, and further kink wave solutions. Herein, we shall exemplify a case for each category of traveling wave solution to facilitate a comparative examination. In alignment with the green curve shown in Fig. 1(d), we derive a periodic wave solution, as depicted in Fig. 4(c)

$$\tilde{u}(x,t) = \frac{\xi_3(\xi_1 - \xi_2)\mathrm{sn}^2(\frac{1}{g}\sqrt{\frac{b}{3}}(x - lt), k) - \xi_1\xi_2 + \xi_2\xi_3}{(\xi_1 - \xi_2)\mathrm{sn}^2(\frac{1}{g}\sqrt{\frac{b}{3}}(x - lt), k) - \xi_1 + \xi_3}. \tag{38}$$

For the blue curve in Fig. 1(d), a bright solitary wave solution of Eq. (3), as illustrated in Fig. 4(f), can be formulated as:

$$\tilde{u}(x,t) = \xi_1 - [\frac{e^{\rho(x-lt)} - 1}{e^{\rho(x-lt)} + 1}]^2(\xi_1 - \xi_2). \tag{39}$$

And considering the blue curve in Fig. 1(j), we can get a kink wave solution (Fig. 5(c)) for KdV equation (3)

$$\tilde{u}(x,t) = \frac{\xi_1 e^{(\xi_1-\xi_2)\sqrt{-\frac{b}{6}}(x-lt)} + \xi_2}{1 + e^{(\xi_1-\xi_2)\sqrt{-\frac{b}{6}}(x-lt)}}. \tag{40}$$

The solutions denoted as Eq. (38), Eq. (39) and Eq. (40)are respectively equivalent to the solutions designated as Eq. (24), Eq. (27) and Eq. (36). By observing the preceding formulas, one can discern that the structures of the solutions for the STFKdV equation and the integer-order KdV equation are quite similar. However, the graphical representations exhibit considerable differences. By observing Fig. 4 and Fig. 5, the following conclusions can be drawn:

1. The solutions of the integer-order KdV equation (3) display a highly regular pattern in their graphical depiction.

2. The graphical representation of the solutions for the fractional-order KdV equation (5) in terms of t closely resembles that of the integer-order KdV equation, with only a slight distortion.

3. The graphical representation of the STFKdV equation (4) concerning both x and t is significantly distorted.

Based on the preceding discussions, we are also able to establish the following theorem:

Theorem V.1. *From a theoretical standpoint, the methodology we have developed is capable of addressing the solution of the entire spectrum of fractional-order KdV equations (4) and (5) under the condition that p is a positive integer.*

Subsequently, we will examine the relationship between the fractional-order KdV equation and the integer-order KdV equation.When $\alpha = 1$ and $\lambda = 1$, then STFKdV equation (4) becomes the integer-order KdV equation (3). It is straightforward to arrive at the following theorem:

Theorem V.2. *The methodology we have developed is capable of addressing the solution of the entire spectrum of integer-order KdV equations (3) under the condition that p is a positive integer.*

VI. Conclusion

In this study, we investigated the space-time fractional-order Korteweg-de Vries (STFKdV) equation using dynamical systems and bifurcation theory. By employing the traveling wave transformation $\eta = x^\lambda - lt^\alpha$, the original fractional-order equation was reduced to a Hamiltonian system, enabling the derivation of exact parametric expressions for traveling wave solutions. Key contributions of this work include:

1) Analytical Solutions: Exact solutions such as periodic waves, bright/dark solitary waves, and kink waves were obtained for both fractional-order ($0 < \alpha, \lambda < 1$) and integer-order ($\alpha = \lambda = 1$) cases. These solutions were expressed in terms of Jacobian elliptic functions and exponential expressions (e.g., Eqs. (24), (27), (36)), demonstrating the structural similarities and graphical differences influenced by fractional parameters.
2) Phase Portrait Analysis: A systematic classification of equilibrium points and bifurcation conditions (e.g., odd vs. even p) was provided, revealing richer dynamical behaviors in fractional-order systems compared to integer-order counterparts (Section III).

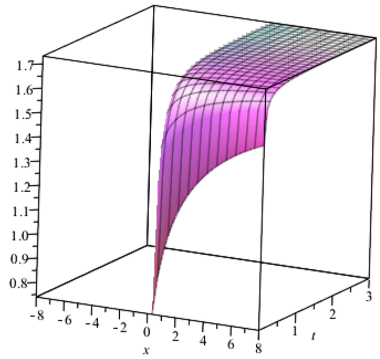

(a) Kink wave solution of (4) with $\alpha = \frac{1}{2}$, $\lambda = \frac{1}{3}$

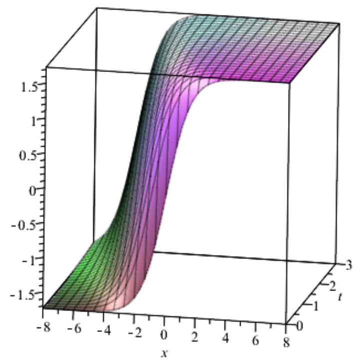

(b) Kink wave solution of (5) with $\alpha = \frac{1}{2}$, $\lambda = 1$

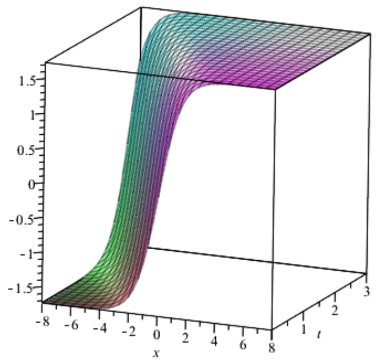

(c) Kink wave solution of (3) with $\alpha = \lambda = 1$

Fig. 5: Graphs of solutions for (3), (4) and (5) $p = 2$, $b = -3$, $c = -3$, $\delta = 0$.

3) Comparative Study: By contrasting the STFKdV equation with the classical KdV equation, we highlighted how fractional parameters α and λ distort wave profiles while preserving solution structures (Section V).

While this study successfully derived analytical solutions and explored bifurcation mechanisms, several aspects require further investigation:

- Parameter Sensitivity Analysis: A systematic numerical evaluation of how fractional parameters (α, λ) and nonlinearity index p quantitatively affect wave amplitude,

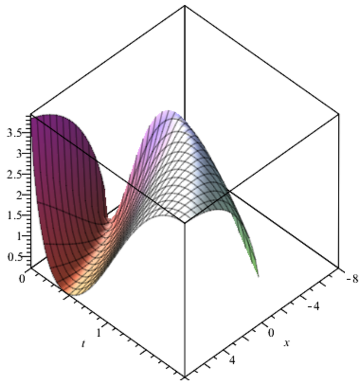

(a) Periodic wave solution of (4) with $\alpha = \frac{1}{2}$, $\lambda = \frac{1}{3}$

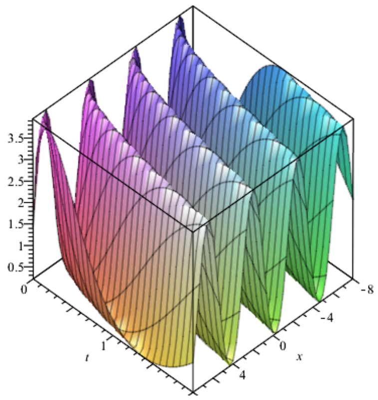

(b) Periodic wave solution of (5) with $\alpha = \frac{1}{2}$, $\lambda = 1$

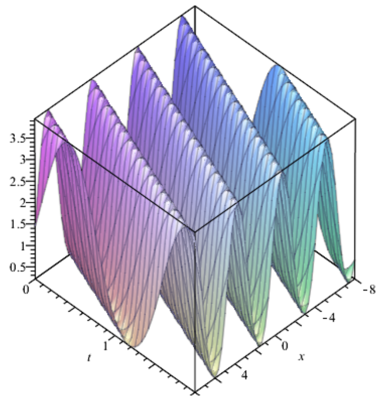

(c) Periodic wave solution of (3) with $\alpha = \lambda = 1$

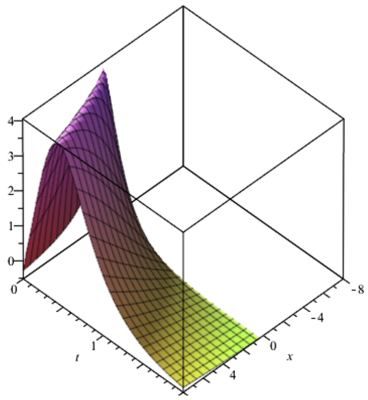

(d) Bright solitary wave solution of (4) with $\alpha = \frac{1}{2}$, $\lambda = \frac{1}{3}$

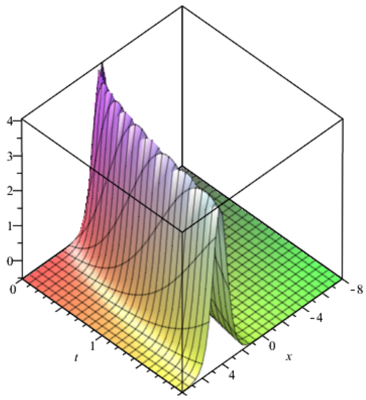

(e) Bright solitary wave solution of (5) with $\alpha = \frac{1}{2}$, $\lambda = 1$

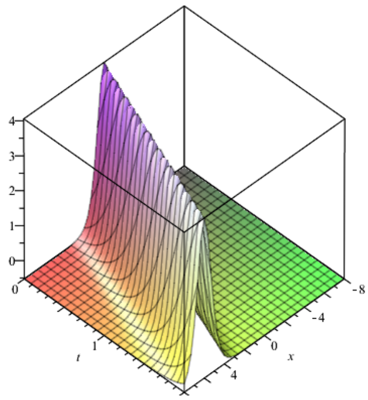

(f) Bright solitary wave solution of (3) with $\alpha = \lambda = 1$

Fig. 4: Graphs of solutions for (3), (4) and (5) with $p = 1$, $b = 3$, $c = 3$, $\delta = 2$.

width, and stability would strengthen the physical relevance of the results.

- Generalization to Higher Dimensions: Extending the methodology to multi-dimensional fractional PDEs (e.g., Kadomtsev-Petviashvili equations) could broaden its applicability.
- Experimental/Numerical Validation: Incorporating numerical simulations (e.g., finite difference methods) or experimental data would validate the derived solutions and enhance practical utility.

REFERENCES

[1] A. Wazwaz, "The variable separated ODE and the tanh methods for solving the combined and the double combined sinh-cosh-Gordon equations," *Appl. Math. Comput,* vol.177, pp745-756, 2006.

[2] A. Wazwaz, "The tanh method for travelling wave solutions to the Zhiber-Shabat equation and other related equations," *Commun Nonlinear Sci. Numer. Simul,* vol.13, no.3, pp584-592, 2008.

[3] W. Ma, Y. Liu, "Invariant subspaces and exact solutions of a class of dispersive evolution equations," *Commun. Nonl. Sci. Numer. Simulat.*, vol.17, no.10, pp3795-3801, 2012.

[4] M. Khater, A. Seadawy, D. Lu, "Optical soliton and rogue wave solutions of the ultra-short femto-second pulses in an optical fiber via two different methods and its applications," *Optik,* vol.158, pp434-450, 2018.

[5] M. Khater, A. Seadawy, D. Lu, "Optical soliton and bright-dark solitary wave solutions of nonlinear complex Kundu-Eckhaus dynamical equation of the ultra-short femtosecond pulses in an optical fiber," *Opt. Quant. Electron.,* vol.50, no.155, pp1-29, 2018.

[6] S. Chen and W. Ma, "Exact solutions to a generalized Bogoyavlensky-Konopelchenko equation via Maple symbolic computations," *Complexity*, vol.2019,no.5, pp8787460, 2019.

[7] H. Zheng, Y. Xia, Y. Bai, L. Guo, "Travelling wave solutions of wuCzhang system via dynamic analysis," *Discrete Dynamics in Nature and Society,* vol.2020, pp2845841, 2020.

[8] R. Attia, D. Lu, T. Ak, M. Khater, "Optical wave solutions of the higher-order nonlinear Schrödinger equation with the non-Kerr nonlinear term via modified Khater method," *Mod. Phys. Lett. B*, vol.34, no.5, pp2050044, 2020.

[9] M. Khater, R. Attia, A. Abdel-Aty, M. Abdou, H. Eleuch, D. Lu, "Analytical and semi-analytical ample solutions of the higher-order nonlinear Schrödinger equation with the non-Kerr nonlinear term," *Results in Physics*, vol.16, pp103000, 2020.

[10] M. Khater, R. Attia, D. Baleanu, "Abundant new solutions of the transmission of nerve impulses of an excitable system," *Eur. Phys. J. Plus*, vol.135, no.2, pp1-12, 2020.

[11] M. Khater, C. Park, A. Abdel-Aty, R. Attia, D. Lu, "On new computational and numerical solutions of the modified Zakharov-Kuznetsov equation arising in electrical engineering," *Alexandria Engineering Journal*, vol.59, no.3, 2020.

[12] M. Khater, C. Park, D. Lu, R. Attia, "Analytical, semi-analytical, and numerical solutions for the Cahn-Allen equation," *Advances in Difference Equations*, vol.2020, no.1, pp1-12, 2020.

[13] J. Li, R. Attia, M. Khater, D. Lu, "The new structure of analytical and semi-analytical solutions of the longitudinal plasma wave equation in a magneto-electro-elastic circular rod," *Modern Physics Letters B*, vol.34, no.12, pp2050123, 2020.

[14] C. Park, M. Khater, R. Attia, W. Alharbi, S. Alodhaibi, "An explicit plethora of solution for the fractional nonlinear model of the low-pass electrical transmission lines via Atangana-Baleanu derivative operator," *Alexandria Engineering Journal*, vol.59, no.3, pp1205-1214, 2020.

[15] H. Zheng, Y. Xia, Y. Bai, L. Wu, "Travelling Wave Solutions of the General Regularized Long Wave Equation," *Qualitative Theory of Dynamical Systems*, vol.20, no.1, pp1-21, 2021.

[16] N. NGbo, Y. Xia, "Traveling wave solution of bad and good modified boussinesq equations with conformable fractional-order derivative,"

Qual. Theory Dyn. Syst. vol.21, no.1, pp1-21, 2022.
[17] Q. Wen, H. Zheng, "Suppressing Chaotic Motion of The Complex Klein-Gordon Equation with External and Parametrical Excitations," *IAENG International Journal of Computer Science*, vol.49, no.4, pp1276-1283, 2022.
[18] W. Yang, "Existence of Positive Steady-state Solution of a Predator-prey Dynamics with Dinosaur Functional Response and Heterogeneous Environment," *Engineering Letters*, vol.31. no.1, pp77-81, 2023.
[19] Q. Cao, K. Djidjeli, W. Price, E. Twizell, "Periodic and chaotic behaviour in a reduced form of the perturbed generalized Korteweg-de Vries and Kadomtsev-Petviashvili equations," *Physica D-nonlinear Phenomena,* vol.125, no.3-4, pp201-221, 1999.
[20] N. Fenichel, "Geometric singular perturbation theory for ordinary differential equations," *Journal Differential Equations*, vol.31, no.1, pp53-98, 1979.
[21] S. Wiggins, *Introduction to applied nonlinear dynamical systems and chaos*. New York: Springer-Verlag, 1990.
[22] G. Derks, S Gils, "On the uniqueness of traveling waves in perturbed Korteweg-de Vries equations," *Japan Journal of Industrial and Applied Matheatics*, vol.10, no.3, pp413-430, 1991.
[23] T. Ogawa, "Traveling wave solutions to a perturbed Koreweg-de Vries equation," *Hiroshima Mathematical Journal*, vol.24, no.2, pp401Ł422, 1994.
[24] E. Fan, H. Zhang, "New exact solutions to a system of coupled KdV equations," *Phys. Lett. A*, vol.245, no.5, pp389-392, 1998.
[25] D. Korteweg, G. Vries, "On the change of form of long waves advancing in a rectangular canal, and on a new type of long stationary waves," *Philosophical Magazine*, vol.91, no.6, pp1007-1028, 2011.
[26] W. Yan, Z. Liu, Y. Liang, "Existence of solitary waves and periodic waves to a perturbed generalized KdV equation," *Mathematical Modelling and Analysis*, vol.9, no.4, pp537-555, 2014.
[27] A. Chen, L. Guo, W. Huang, "Existence of kink waves and periodic waves for a perturbed defocusing mKdV equation," *Qualitative Theory of Dynamical Systems*, vol.7, no.3, pp495-517, 2018.
[28] X. Sun,W. Huang, "Coexistence of the solitary and periodic waves in convecting shallow water fluid," *Nonlinear Analysis: Real Word Applications*, vol.53, pp103067, 2020.
[29] A. Chen, C. Zhang, W. Huang, "Monotonicity of limit wave speed of traveling wave solutions for a perturbed generalized KdV equation," *Applied Mathematics Letters*, vol.121, pp107381, 2021.
[30] H. Liu, C. Bai, X. Xin, X. Li, "Equivalent transformations and exact solutions to the generalized cylindrical KdV type of equation," *Nuclear Physics B* vol.952, pp114924, 2020.
[31] H. Liu, B. Sang, X. Xin, "CK transformations, symmetries, exact solutions and conservation laws of the generalized variable-coefficient KdV types of equations," *Comput. Appl. Math.*vol.345, pp127-134, 2019.
[32] H. Liu, L. Zhang, X. Li, L. Chang, "Equivalent transformations, bifurcations and exact solutions to a class of variable-coefficient PDE," *Nuclear Physics B* vol.960, pp115172, 2020.
[33] R. Khalil, M. Al Horani, A. Yousef, and M. Sababheh, "A new definition of fractional derivative," *Journal of Computational and Applied Mathematics,* vol.264, pp65-70, 2014.
[34] J. Li. *Singular Nonlinear Travelling Wave Equations: Bifurcations and Exact Solutions*. Beijing: Science, 2013
[35] P. Byrd and M. Friedman. *Handbook of Elliptic Integrals for Engineers and Scientists*. New York: Springer-Verlag, 1971.